

PCCP

Accepted Manuscript

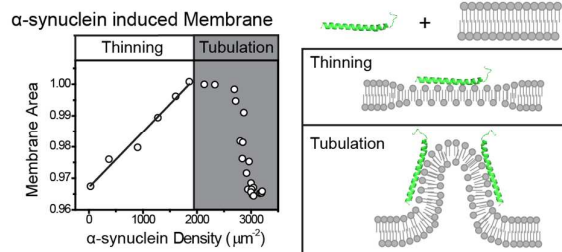


This is an *Accepted Manuscript*, which has been through the Royal Society of Chemistry peer review process and has been accepted for publication.

Accepted Manuscripts are published online shortly after acceptance, before technical editing, formatting and proof reading. Using this free service, authors can make their results available to the community, in citable form, before we publish the edited article. We will replace this *Accepted Manuscript* with the edited and formatted *Advance Article* as soon as it is available.

You can find more information about *Accepted Manuscripts* in the [Information for Authors](#).

Please note that technical editing may introduce minor changes to the text and/or graphics, which may alter content. The journal's standard [Terms & Conditions](#) and the [Ethical guidelines](#) still apply. In no event shall the Royal Society of Chemistry be held responsible for any errors or omissions in this *Accepted Manuscript* or any consequences arising from the use of any information it contains.

Table of contents**Colour graphic:****One sentence highlight (<20 words):**

α -synuclein leads to thinning, and subsequent tubulation of membrane bilayer.

Cite this: DOI: 10.1039/c0xx00000x

www.rsc.org/xxxxxx

ARTICLE TYPE

Biophysics of α -synuclein induced membrane remodelling

Zheng Shi^a, Jonathan Sachs^b, Elizabeth Rhoades^c and Tobias Baumgart^{*a}

Received (in XXX, XXX) Xth XXXXXXXXXX 20XX, Accepted Xth XXXXXXXXXX 20XX

DOI: 10.1039/b000000x

α -synuclein is an intrinsically disordered protein whose aggregation is a hallmark of Parkinson's disease. In neurons, α -synuclein is thought to play important roles in mediating both endo- and exocytosis of synaptic vesicles through interactions with either the lipid bilayer or other proteins. Upon membrane binding, the N-terminus of α -synuclein forms a helical structure and inserts into the hydrophobic region of the outer membrane leaflet. However, membrane structural changes induced by α -synuclein are still largely unclear. Here we report a substantial membrane area expansion induced by the binding of α -synuclein monomers. This measurement is accomplished by observing the increase of membrane area during the binding of α -synuclein to pipette-aspirated giant vesicles. The extent of membrane area expansion correlates linearly with the density of α -synuclein on the membrane, revealing a constant area increase induced by the binding per α -synuclein molecule. The area expansion per synuclein is found to exhibit a strong dependence on lipid composition, but is independent of membrane tension and vesicle size. Fragmentation or tubulation of the membrane follows the membrane expansion process. However, contrary to BAR domain proteins, no distinct tubulation-transition density can apparently be identified for α -synuclein, suggesting a more complex membrane curvature generation mechanism. Consideration of α -synuclein's membrane binding free energy and biophysical properties of the lipid bilayer leads us to conclude that membrane expansion by α -synuclein results in thinning of the bilayer. These membrane thinning and tubulation effects may underlie α -synuclein's role in mediating cell trafficking processes such as endo- and exocytosis.

Introduction

α -synuclein has been widely studied for its crucial role in Parkinson's disease. This intrinsically disordered protein forms a shallowly inserted amphipathic helix after binding to a membrane bilayer containing negatively charged lipids, and this binding can lead to membrane remodelling¹⁻⁴. Significant efforts using a wide range of different techniques have been dedicated to elucidating the membrane remodelling ability of α -synuclein. In EM studies, vesicles were observed to deform into cylindrical tubes or micelles when co-incubated with α -synuclein⁵⁻⁸. AFM, NMR as well as X-ray scattering studies, have indicated α -synuclein to stretch the bilayer upon binding and therefore to induce membrane-thinning⁹⁻¹¹. However, the underlying mechanisms and connections between these biophysical phenomena are still missing.

In neurons, α -synuclein has a concentration of tens of micromolars and is speculated to modulate the fusion of synaptic vesicles into the plasma membrane¹²⁻¹⁶. Recent experiments also suggest that α -synuclein plays a positive role in the early steps of endocytosis¹⁷. Therefore, elucidating the mechanism of α -synuclein membrane interaction is a critical step towards understanding the physiological and pathological functions of α -synuclein.

Here, the membrane remodelling ability of α -synuclein is studied

on individual giant unilamellar vesicles (GUVs). A substantial membrane area expansion is observed followed by fragmentation or tubulation of the membrane. The extent of membrane expansion correlates linearly with the α -synuclein density on the GUV, resulting in an area expansion per synuclein molecule larger than the area of the membrane binding site of the protein. The area expansion constant is independent of membrane tension and vesicle size, indicating that the expansion phenomenon is not a result of the protein's effect on the membrane undulation (out-of-plane fluctuation) spectrum. However, a strong dependence of the area expansion constant on lipid composition is observed, with a significantly larger expansion effect (per protein molecule) on a cell mimicking lipid composition than on membranes composed only of DOPS. We used a fluorescence quenching assay to confirm that lipid flip-flop across the bilayer is not significantly enhanced in the presence of α -synuclein, implying that the area expansion effect is related to membrane thinning as opposed to the redistribution of lipids across the bilayer due to asymmetric α -synuclein insertion.

Significant membrane thinning effects have been found for many membrane interacting peptides or proteins¹⁸⁻²⁰. To our knowledge, however, the contribution from individual molecules has not yet been quantified either due to inherent limits of the technique used or due to a nonlinear thinning behaviour found for several

peptides^{20, 21}. Finally, in addition to membrane expansion, our experimental approach allows us to monitor tubulation transitions following the area expansion process. Membrane expansion and tubulation are likely two interrelated α -synuclein membrane interaction modes operating in different α -synuclein density regimes. We believe our results enhance the understanding of α -synuclein membrane interactions and provide useful insights in understanding the biological roles of this protein.

Experimental section

Materials

Lipids 1,2-dioleoyl-sn-glycero-3-phosphocholine (DOPC), 1,2-dioleoyl-sn-glycero-3-phospho-L-serine (DOPS), 1,2-dioleoyl-sn-glycero-3-phosphoethanolamine (DOPE), and 1-palmitoyl-2-oleoyl-sn-glycero-3-phosphocholine (POPC) were obtained from Avanti Polar Lipids (Alabaster, AL). Alexa Fluor® 488 (AF-488) C5-maleimide, BODIPY® FL DHPE (N-(4,4-Difluoro-5,7-Dimethyl-4-Bora-3a,4a-Diaza-s-Indacene-3-Propionyl)-1,2-Dihexadecanoyl-sn-Glycero-3-Phosphoethanolamine, Triethylammonium Salt), NBD-PE (N-(7-Nitrobenz-2-Oxa-1,3-Diazol-4-yl)-1,2-Dihexadecanoyl-sn-Glycero-3-Phosphoethanolamine, Triethylammonium Salt) and Texas Red-1,2-dihexadecanoyl-sn-glycero-3-phosphoethanolamine (Triethylammonium salt) were from Life Technologies (Grand Island, NY). Na₂S₂O₄ (SDT), casein, Tris, HEPES, and EDTA were obtained from Fisher Scientific (Rochester, NY). All commercial reagents were used without further purification.

Protein purification

N-terminally acetylated α -synuclein bearing an S9C mutation (mol. wt. = 14.5 kDa) was expressed, purified and then labelled with Alexa-488 maleimide at S9C as previously described^{22, 23}. ENTH_GFP was expressed and purified following ref²⁴. Both proteins were stored at -80 °C after purification. Thawed proteins were kept on ice before fluorescence imaging. All measurements were taken within five days after thawing the protein.

Imaging chamber preparation and GUV transfer procedures

GUVs were prepared by electroformation in 300mM sucrose solution with 0.3% Texas Red-DHPE in desired lipid compositions as previously described²⁵. Two imaging compartments, a GUV chamber and a protein chamber, were formed between two coverslips (20mm×40mm, pre-treated with 2μL of 2.5mg/ml casein, 20mM Tris, and 2mM EDTA) overhanging a glass microscope slide (2mm thick)²⁶. The GUV chamber had a total volume of 375μL and was made by diluting 5~15μL of the GUV stock solutions into a buffer containing glucose, sucrose, NaCl and HEPES. The osmolarity of the buffer was selected to be 20% higher than the GUV stock solution (measured with a micro-osmometer Advanced Instruments Inc. (Norwood, MA)) to ensure that the vesicles had enough excess area for micropipette aspiration. The protein chamber had a total volume of 187.5μL. The protein stock solution was diluted to designated concentrations, using the same buffer as used for diluting GUVs. For both chambers, we chose pH = 7 and NaCl was kept at 50mM, with 7mM HEPES. Sucrose and glucose (1:1) concentrations were adjusted to yield total osmolarities of the

desired values. Micropipettes and transfer capillaries were prepared and casein-treated as described^{25, 27}. GUVs were pre-stretched under a membrane tension >0.5mN/m before step 2 of the transfer process (Fig.1). Zero aspiration pressure was checked before and after the protein-GUV association process to ensure absence of pressure drifts²⁸. All the transfer and imaging processes were carried out at room temperature (24 °C).

Microscopy and data analysis

The protein-membrane association process and the membrane geometry changes were monitored with a confocal fluorescence microscope²⁵, using a 60x 1.1 N.A. objective (Olympus, Center Valley, PA). The aspiration length, L_p , micropipette radius, R_p and GUV radius, R_v were measured with Image J, as illustrated in Figure 1a. The GUV geometry was calculated as $Area(t) = 4\pi R_v(t)^2 + 2\pi R_p L_p(t)$, $Volume(t) = 4\pi R_v(t)^3/3 + \pi R_p^2 L_p(t)$. The average protein fluorescence intensity was determined by fitting a Gaussian ring to the GUV contour (excluding the aspirated region) using MATLAB. R_v could also be obtained from the fitting and was double-checked through direct measurement via Image J.

The measured fluorescence intensity was then converted into a protein monomer density $\rho(t)$ following Ref.²⁹. GUVs containing x% BODIPY and (100-x)% DOPC were prepared (x: 0.1~2) and at least 20 independent GUVs were imaged under the same settings as during the recording of GUV-protein association. A linear fit ($r^2=0.99$) was carried out to obtain the relation between measured GUV fluorescence intensity and BODIPY density on the membrane. The quantum yield difference between BODIPY and AF-488 was determined to be $BODIPY/AF-488=0.5$, by imaging bulk solution intensity of SUVs (containing BODIPY) and AF-488 labelled proteins under the same solution conditions as in our experiments (50mM NaCl, pH 7)³⁰. The average lipid headgroup area was assumed as 0.7 nm².

The membrane instability point t_c was defined as the time point when $Area(t)$ begins to decrease, and the corresponding protein density $\rho(t_c)$ was defined as the instability transition-density.

Fig. 1 Experimental Method:

Membrane shape transitions studied by single GUV transfer method. a) A schematic representation of a pipette-aspirated GUV. R_v and R_p are the radii of the GUV and aspiration pipette respectively. L_p is the aspiration length, ΔP is the aspiration pressure. b) The process of transferring a single GUV from a GUV dispersion (red) to a protein solution (green) (See reference³¹ for more details). During the binding of α -synuclein onto the transferred GUV, membrane area and protein density on the membrane (determined from the protein's fluorescence intensity) were monitored simultaneously.

Zeta potential measurements

We measured the electrophoretic mobility of LUVs under the same experimental conditions as in other experiments with a Delsa Nano C Particle Analyzer. The Helmholtz-Smoluchowski relation was used to convert the measured mobility to zeta potential. LUVs (DOPS/DOPE/DOPC=45/30/25, or pure DOPS) were prepared in 300mM sucrose and extruded 23 times with 100nm pore size filters. Each measurement was repeated three times.

Fluorescence spectroscopy

LUVs (99%DOPS and 1%NBD-PE) were prepared in 300mM sucrose and extruded 23 times with 100nm pore size filters.

Fluorescence signals of NBD were collected with a Cary Eclipse fluorometer with single wavelength excitation at 463nm for LUV solutions under various experimental conditions. Peaks of the emission spectra (at 536nm) were used to calculate the amount of fluorescence quenching in the presence of Na₂S₂O₄ (SDT).

Results and discussion

Binding of α -synuclein linearly increases the membrane area

To study the α -synuclein induced membrane-remodelling process, we employed a single GUV analysis method recently developed by us (Fig. 1)^{26, 27}. Briefly, individual pipette-aspirated GUVs were transferred into solutions containing a fixed concentration of α -synuclein monomers. GUV area and α -synuclein density on the membrane were recorded simultaneously once the vesicle is exposed to the α -synuclein solution. As shown in Fig. 2a, the binding of α -synuclein is accompanied by an increase of the GUV's pipette aspiration length as well as a dilution of lipid dye in the membrane (Fig. S1), indicating an expansion of the membrane through α -synuclein binding. Analysis of the protein density and GUV area (Fig. 2b, Fig. S1a, also see Methods) results in a linear relation between these two quantities (Fig. 2c).

The area expansion constant (the amount of area expansion induced by the binding of one α -synuclein molecule) can therefore be determined from a linear fit as shown in Fig. 2c. For pure DOPS GUVs in a 250nM α -synuclein solution, the area expansion constant is found to be $22.2 \pm 5.4 \text{ nm}^2$ (Mean \pm SD from 24 GUVs), which is slightly larger than the size of the membrane-binding site of α -synuclein determined from molecular dynamic simulation studies (about 15 nm^2)¹¹. The linearity between α -synuclein density and membrane area expansion clearly indicates that when expanding the bilayer, contributions from individual α -synuclein molecules are linearly additive. In other words, protein cooperativity on the membrane does not contribute significantly to the membrane expansion under situations we consider here. Molecular dynamics studies comparing the membrane remodelling abilities of single versus multiple α -synucleins demonstrated similar additive behaviour¹¹. However, this is not a universal feature of protein/peptide induced membrane expansions. For example, non-linear area-density relations were observed when the same experiment was repeated for ENTH domains (Fig. S2), and no expansion effect was observed for the endophilin N-BAR domain²⁶. Both of these proteins are endocytic accessory proteins with well documented membrane insertion abilities³².

Fig.2 Binding of α -synuclein linearly expands the membrane

a) Time lapse confocal images showing the change of membrane area during α -synuclein binding. The GUV consists of 99.7%DOPS and 0.3%TexasRed-DHPE. Membrane tension was held constant at 0.15mN/m. Green: protein channel; red: lipid channel. Scale bar: 10 μ m. b) Measured protein density on membrane (black) and GUV membrane area (blue) from the recorded confocal images shown in a). c) A linear fit ($r^2=0.963$) of the membrane area (normalized to the initial membrane area) to α -synuclein density on the membrane as shown in b), the resulting slope is defined as the 'area expansion constant'.

α -synuclein causes a significantly larger expansion per molecule on a more biologically relevant membrane composition

Biological membranes have an extremely complicated lipid composition: besides PS lipids, PE and PC lipids are present in the cytosolic leaflet of plasma membrane, in addition to a large range of minority lipids³³. We therefore seek to answer if the area expansion effect we observed on pure DOPS membrane is also present on a more biologically relevant lipid composition, with a composition of DOPS/DOPE/DOPC = 45/30/25.

Fig. 3 The area expansion constant is significantly larger on GUVs with plasma membrane mimicking lipid composition.

a) Representative area-density relations for pure DOPS GUVs (open) and GUVs with DOPS/DOPE/DOPC=45/30/25 (closed). Solid lines are linear fits of the normalized area with respect to α -synuclein density on the membrane. b) The area expansion constant of α -synuclein is significantly larger on DOPS/DOPE/DOPC=45/30/25 membranes (average of 8 GUVs) than on pure DOPS GUVs (average of 25 GUVs). Black error bars are SEM, grey error bars are SD. Student t-test, *** $p < 0.001$. The comparison is carried out under the same bulk protein concentration (250nM).

As expected, a significantly lower amount of α -synuclein can associate onto the biologically more relevant composition. This agrees with the facts that α -synuclein membrane interaction is dominated by electrostatics¹, and that the zeta-potentials³⁴ that we determined have values of $-50.7 \pm 2.3 \text{ mV}$ (Mean \pm SD) for the composition of DOPS/DOPE/DOPC = 45/30/25, and $-65.7 \pm 2.6 \text{ mV}$ (Mean \pm SD) for pure DOPS membrane. However, as shown in Fig. 3a, similar total area increase can be achieved on both types of membranes, resulting in an area expansion constant significantly larger on membranes with PE and PC than on the pure PS membrane (Fig. 3b). Therefore, we expect the membrane area expansion induced by α -synuclein binding to be an important effect in cellular events, with the amount of expansion by individual α -synuclein molecules significantly larger than its cross-section area on the membrane¹¹. The membrane with more biological lipid composition may have a smaller transverse elastic modulus compared to the pure DOPS membrane. This could contribute to the much larger area expansion constant observed on the DOPS/DOPE/DOPC = 45/30/25 GUVs as will be discussed later. α -synuclein may also reduce the lateral expansion of PS lipids due to the stronger interaction between the protein and the charged PS headgroup. Therefore, the smaller amount of PS on the cell mimicking GUV could be another source for the larger area expansion effect. As for distinguishing the contributions of PE and PC to the membrane area expansion, unfortunately, α -synuclein binds very weakly on GUVs with DOPS/ DOPC=45/55 (protein density change $< 200 \mu\text{m}^2$), making it impossible to accurately measure the area expansion constant on this lipid composition with only PC and PS (Fig. S3).

Membrane expansion induced by α -synuclein is a reversible process

We then asked if the membrane expansion induced by α -synuclein is reversible, that is, whether membrane area will decrease when α -synuclein molecules unbind from the membrane. To measure this, we transferred α -synuclein bound GUVs into a large volume of buffer solution containing small vesicles devoid

of any α -synuclein. As expected, the GUV area decreases during α -synuclein dissociation, with a linear relation between the protein density and membrane area (Fig. 4). The resulting area expansion constant qualitatively agrees with the value determined from α -synuclein membrane association studies (Fig. 3).

Fig. 4 The membrane area decreases during α -synuclein dissociation.

a) GUVs (DOPS/DOPE/DOPC=45/30/25) pre-incubated with α -synuclein were transferred into a bulk solution of 50 μ g/ml SUVs (diameter=50nm, 100%DOPS). A decrease in membrane area (blue) was found to accompany the dissociation process of α -synuclein (black). Time zero is defined as the time point when the α -synuclein covered GUV is exposed to the SUV solution. b) Linear fit of the normalized area with respect to α -synuclein density. The resulting area expansion constant of 62nm² per molecule is comparable to what was observed for the α -synuclein association process, see Figure 3 (73 \pm 12nm² per molecule, Mean \pm SD).

A variety of protein membrane interaction processes can lead to an increase in GUV membrane area. These could include: the formation membrane pores; direct stretching or thinning of the lipid bilayer; smoothening of membrane undulations due to protein binding; protein membrane insertion followed by a rapid lipid flip-flop. To elucidate the underlying mechanism of α -synuclein induced membrane expansion, we next aim to discuss all of the scenarios considered above.

The formation of pores (larger than the size of α -synuclein) on the GUV can be easily excluded simply based on the fact that fluorescent α -synuclein cannot diffuse across the bilayer (Fig. S4) and that the GUV remains intact during the area expansion process (Fig. 1, Fig. 7b and Fig. S2b). In the following, we will focus on discussions regarding the interference of α -synuclein with: membrane undulation, transmembrane dynamics of lipids, membrane stretching, and membrane thinning. In order to achieve an accurate estimate of the area expansion constant, a large range of α -synuclein density change during protein-membrane association is required (Fig. S5). Therefore, in the following quantitative analyses, experiments were performed on GUVs comprised only of DOPS where typically an α -synuclein density change larger than 2000 μ m⁻² can be observed during the protein-membrane association process.

The membrane expansion effect does not represent α -synuclein's effect on membrane undulations

Due to thermal fluctuations, a certain area fraction of freely suspended membranes is always stored as surface undulations which are typically beyond the spatiotemporal resolution of our technique²⁶. The amount of membrane undulation is inversely related to the membrane bending rigidity and tension. Consequently, an increase in the observed membrane area will happen when the binding of protein stiffens the membrane or locally increases membrane tension³⁵. Therefore, the observed area expansion effect may represent interference between α -synuclein and the membrane fluctuation spectrum.

In this scenario, one should expect the area expansion constant to be directly dependent on the initial global membrane tension adjusted by the aspiration pipette. That is, a smaller area expansion constant is expected on GUVs of higher membrane tension (which show less undulation).

However, from our experimental data, no clear dependence can be identified between the area expansion constant and membrane tension (Fig. 5a). In fact, a linear fit of the area expansion constant to membrane tension yields a zero slope within statistical error. Therefore we conclude that the area expansion is not a result of smoothing out membrane undulation by α -synuclein membrane binding. We mention in passing that no dependence of the area expansion constant on the GUV radius can be observed either (Fig 5b).

Fig.5 Area expansion by α -synuclein is independent of membrane tension and vesicle size

a) Measured area expansion constant for GUVs under various membrane tensions. b) Measured area expansion constant for GUVs of different sizes. The solid lines represent the linear fit of the area expansion constant to the membrane tension in a) or to the GUV radius in b). In both cases, the slope of the linear fit is zero within statistical error. (0 \pm 10pL/N in a) and -0.1 \pm 0.2pm in b)). Error bars are the standard errors in determining the area expansion constant. Protein concentration was 250nM.

The membrane expansion effect does not represent α -synuclein's effect on trans-membrane lipid flip-flop dynamics

Membrane associated α -synuclein inserts shallowly into only one leaflet of the bilayer (the outer leaflet of the vesicle in the case of our experiments)^{4, 36}. The enhanced pressure within the outer leaflet has been speculated to be one of the major driving forces for the formation of external membrane protrusions³².

If the membrane expansion we observed is a direct result of α -synuclein membrane insertion, two consequences should be expected. First, the amount of area expansion by individual molecules would be similar to, or smaller than, the size of α -synuclein membrane binding site. Secondly, in order to expand the two leaflets simultaneously, there would have to be a pathway through which lipids can flip across the bilayer within our time resolution (about 4 seconds)³⁷.

Contrary to the first expectation, however, the measured area expansion constant is larger than the size of membrane binding site, especially on the plasma membrane mimicking GUVs. This indicates that the observed membrane expansion is not achieved merely by α -synuclein insertion.

Through lipid flip-flop, the area asymmetry induced by α -synuclein insertion can be released, resulting in an increase in bilayer membrane area³⁷. The trans-membrane flip-flop rate is extremely slow for phospholipid bilayers³⁸. Therefore, to test the second expectation, we investigate whether the presence of membrane bound α -synuclein can greatly enhance the trans-membrane dynamics of lipids.

To achieve this, we used a classical quenching assay based on the dye NBD-PE, which was incorporated homogeneously into 100nm DOPS LUVs. The fluorescence of NBD-PE was irreversibly quenched in the presence of Na₂S₂O₄ (SDT), a chemical which does not permeate the lipid bilayer³⁸. Therefore, when SDT is added into NBD-PE containing LUVs, dyes on the outer leaflets of the vesicles will be quenched, leading to a roughly 50% reduction of the total fluorescence signal. Furthermore, a nearly 100% quenching of fluorescence is expected if α -synuclein were to swiftly flip the lipids, thereby

exposing NBD originally on the inner leaflets to the fluorescence quencher. However, much weaker effects were observed in the presence of α -synuclein, similar to that of casein, a cytosolic protein which is inert to lipid membranes (Fig. 6). Therefore, membrane binding of α -synuclein does not promote lipid flip-flop across the bilayer under our experimental conditions, and the insertion of α -synuclein is unlikely to play an important role in the membrane expansion observed here.

Fig.6 The membrane binding of α -synuclein does not promote lipid flip-flop in bilayer.

a) Fluorescence measurement of 0.1 mg/ml LUVs containing NBD-PE (99%DOPS + 1% NBD-PE, 100nm diameter) co-incubated with buffer (30mM NaCl in 150mM Tris, black), SDT (15mM SDT in 150mM Tris, red), or with further addition of α -synuclein (0.04 mg/ml, green), casein (0.04mg/ml, blue), or detergent (2% v/v, gray). All concentrations refer to the final concentration of the species used for fluorescence measurements. b) Summary of the NBD fluorescence quenching results. The addition of α -synuclein does not induce significant further quenching of NBD as in the case of adding detergent. No significant difference can be found after the addition of α -synuclein and between the effects of α -synuclein and casein by a Student t-test (N.S.: $p>0.1$).

The membrane expansion effect is most likely a result of α -synuclein induced membrane thinning

Having eliminated the possibility that our observed area expansion is a result of α -synuclein interfering with membrane undulations or lipid trans-membrane dynamics, we next discuss the possibility of a role for α -synuclein in directly stretching or thinning the bilayer. The membrane binding free energy ΔG of an α -synuclein molecule on negatively charged membranes can be calculated from a published value of the α -synuclein membrane binding constant K_D (in terms of lipid concentration). We estimated the membrane binding energy as $\Delta G = -k_B T \ln(K_D/n) = 16k_B T$, where $K_D = 2.25\mu\text{M}$ and $n=23$ is the number of lipids bound by one α -synuclein molecule³⁹. This binding free energy sets an upper limit for the amount of energy α -synuclein molecules can utilize to expand the bilayer. Lipid bilayers are comparatively hard to directly stretch (via increasing the lipid distance via application of a lateral force). Considering the typical membrane stretch elastic modulus ($E_{xx}=0.2\text{ N/m}^{40}$), it can be seen that an energy of more than 1000 $k_B T$ is required for stretching an area of 22nm^2 per molecule (the area expansion constant measured on DOPS GUVs) out of the bilayer. Therefore, the area increase we observed cannot be the result of direct membrane stretching.

On the other hand, the transverse elastic modulus of membrane bilayers E_{zz} , which describes the change in membrane thickness upon applying a force vertical to the membrane surface, is typically between 0.4~4 MPa⁴¹. The membrane binding energy of one α -synuclein molecule can lead to a squeezing of a piece of membrane originally with thickness d and area a by

$$\Delta d = -\Delta G / (aE_{zz}) \quad (1)$$

Assuming conservation of lipid volume, the reduction in membrane thickness should be directly correlated with an expansion of the membrane area Δa

$$\Delta a = \frac{ad}{\left[d - \frac{\Delta G}{aE_{zz}}\right]} - a \quad (2)$$

Typical bilayers are about 4nm thick and molecular dynamic simulations indicate that individual α -synuclein molecules usually act upon a membrane area of about 50nm^2 ¹¹. Taking $a=50\text{nm}^2$ and $d=4\text{nm}$ in equation (2), the binding energy of one α -synuclein monomer can potentially induce an area expansion of $4\sim 240\text{nm}^2$. Notably, our experimentally measured area expansion constants do fall into this range.

Interestingly, a recent study hypothesized that α -synuclein can expand the membrane through inducing lipid interdigitation⁹. The binding energy of α -synuclein is sufficient to enable squeezing a 50nm^2 bilayer into a compact monolayer, thereby inducing an area expansion of about 50nm^2 ^{42,43}, which is, again, in agreement with our results. In summarizing these considerations, we conclude that the membrane expansion we observed is most likely a result of α -synuclein induced membrane thinning.

Membrane tubulation or fragmentation follows the area expansion process

α -synuclein has been reported to induce dramatic membrane remodelling such as tubulation and total fragmentation of the membrane *in vitro*⁵⁻⁸. Indeed, in our hands GUVs containing pure DOPS almost always collapse after a certain amount of area expansion (Fig. 7a, 7e). In our setup, the initiation of high curvature membrane tubes can be revealed by a decrease in apparent GUV area. For BAR domain proteins, this phenomenon has been well described by a linear curvature instability theory²⁶. Briefly, GUVs under certain membrane tensions become tubulated when protein densities on the membrane reach a critical level. However, for α -synuclein, membrane area reduction, and thereby tubulation, was only observed on a small fraction of GUVs after the initial area expansion process (Fig. 7b-e). Therefore, the underlying mechanism of α -synuclein induced membrane tubulation may be more complex than that of BAR domain proteins. One reason for this complication might be related to the initial thinning phase during the α -synuclein membrane interaction. If the membranes are initially thinned by the binding of α -synuclein, the bilayer may become interdigitated and eventually form cylindrical micelles as oppose to membrane tubes⁵.

Regardless of the complexity of the mechanism, our results clearly demonstrate that α -synuclein-induced membrane tubulation only occurs after a thinning phase of the bilayer. This in fact has important biological implications since the ability to generate membrane curvature is directly related to the potential roles of α -synuclein in mediating endocytosis. Moreover, membrane thinning can lower the membrane bending modulus²⁰. This effect is in turn expected to affect the functions of other membrane curvature generating proteins. The influence of α -synuclein on vesicle trafficking processes will be a topic for future research.

Fig.7 α -synuclein induced membrane fragmentation/ tubulation proceeds after area expansion (on pure DOPS GUVs)

a) Time lapse confocal images showing the fragmentation of the outer bilayer of a double-bilayer vesicle during α -synuclein binding. b) Time lapse confocal images showing the decrease of membrane area following the initial membrane expansion effect during α -synuclein binding. c) Analysis of the α -synuclein density and corresponding membrane area

change for a GUV showing area reduction due to membrane tubulation. d) Area-density relation for c), a linear fit to the area increasing phase yielded an area expansion of 18nm² per molecule, in agreement with the value obtained from GUVs which showed only an area expansion phase during α -synuclein association (22.2 ± 5.4nm² per α -synuclein, Mean ± SD from 24 GUVs). e) Diagram summarizing the α -synuclein induced membrane remodeling. Open circles represent the maximal α -synuclein density (fragmentation density) on GUVs that only showed membrane expansion (i.e. no tubulation). Black triangles represent transition densities of α -synuclein on GUVs showing area reduction through tubulation. GUV composition: 99.7%DOPS, 0.3% Texas Red-DHPE.

In summary, we found substantial membrane thinning induced by α -synuclein binding. We also demonstrated that membrane tubulation can occur after the initial membrane thinning process as an additional α -synuclein membrane interaction mode. Therefore, our measurements complement previous observations regarding the membrane remodelling properties of α -synuclein^{5, 8-10} and can provide useful insights for future research towards understanding how α -synuclein affects vesicle trafficking processes.

Acknowledgements

We are grateful for funding from NSF grant CBET 1053857 (T.B.) and NIH grants GM 097552 (T.B.), GM102815 (E.R.), and NS084998 (J.S). Furthermore we thank Mike Lacy for providing fluorescently labelled α -synuclein samples, and Dr. Jeffery Saven for providing access to the fluorometer.

^a Department of Chemistry, University of Pennsylvania, Philadelphia, PA 19104, USA

^b Department of Biomedical Engineering, University of Minnesota Twin Cities, Minnesota, MN 55455, USA

^c Department of Molecular Biophysics and Biochemistry, Yale University, New Haven, CT 06511, USA

*To whom correspondence should be addressed: T. Baumgart,

³⁵ Department of Chemistry, University of Pennsylvania, 231 South 34th Street, 19104, Philadelphia, PA, USA, Tel.: 215 573 7539; E-mail: baumgart@sas.upenn.edu

† Electronic Supplementary Information (ESI) available: Figures S1-S5. See DOI: 10.1039/b000000x/

References

1. E. Rhoades, T. F. Ramlall, W. W. Webb and D. Eliezer, *Biophysical Journal*, 2006, **90**, 4692-4700.
2. A. J. Trexler and E. Rhoades, *Biochemistry*, 2009, **48**, 2304-2306.
3. M. Robotta, P. Braun, B. van Rooijen, V. Subramaniam, M. Huber and M. Drescher, *Chemphyschem*, 2011, **12**, 267-269.
4. I. M. Pranke, V. Morello, J. Bigay, K. Gibson, J. M. Verbavatz, B. Antony and C. L. Jackson, *Journal of Cell Biology*, 2011, **194**, 88-102.
5. N. Mizuno, J. Varkey, N. C. Kegulian, B. G. Hegde, N. Q. Cheng, R. Langen and A. C. Steven, *Journal of Biological Chemistry*, 2012, **287**, 29301-29311.
6. C. H. Westphal and S. S. Chandra, *Journal of Biological Chemistry*, 2013, **288**, 1829-1840.
7. J. Varkey, J. M. Isas, N. Mizuno, M. B. Jensen, V. K. Bhatia, C. C. Jao, J. Petrlova, J. C. Voss, D. G. Stamou, A. C. Steven and R. Langen, *Journal of Biological Chemistry*, 2010, **285**, 32486-32493.
8. Z. Jiang, M. de Messieres and J. C. Lee, *Journal of the American Chemical Society*, 2013, **135**, 15970-15973.
9. M. M. Ouberai, J. Wang, M. J. Swann, C. Galvagnion, T. Williams, C. M. Dobson and M. E. Welland, *Journal of Biological Chemistry*, 2013, **288**, 20883-20895.
10. A. Leftin, C. Job, K. Beyer and M. F. Brown, *Journal of Molecular Biology*, 2013, **425**, 2973-2987.
11. A. R. Braun, E. Sevcsik, P. Chin, E. Rhoades, S. Tristram-Nagle and J. N. Sachs, *Journal of the American Chemical Society*, 2012, **134**, 2613-2620.
12. B. G. Wilhelm, S. Mandad, S. Truckenbrodt, K. Kröhnert, C. Schäfer, B. Rammner, S. J. Koo, G. A. Claßen, M. Krauss, V. Haucke, H. Urlaub and S. O. Rizzoli, *Science*, 2014, **344**, 1023-1028.
13. D. C. DeWitt and E. Rhoades, *Biochemistry*, 2013, **52**, 2385-2387.
14. J. Burre, M. Sharma, T. Tsetsenis, V. Buchman, M. R. Etherton and T. C. Sudhof, *Science*, 2010, **329**, 1663-1667.
15. J. J. Diao, J. Burre, S. Vivona, D. J. Cipriano, M. Sharma, M. Kyoung, T. C. Sudhof and A. T. Brunger, *Elife*, 2013, **2**.
16. B. K. Choi, M. G. Choi, J. Y. Kim, Y. Yang, Y. Lai, D. H. Kweon, N. K. Lee and Y. K. Shin, *Proceedings of the National Academy of Sciences of the United States of America*, 2013, **110**, 4087-4092.
17. K. J. Vargas, S. Makani, T. Davis, C. H. Westphal, P. E. Castillo and S. S. Chandra, *Journal of Neuroscience*, 2014, **34**, 9364-9376.
18. H. W. Huang, *Biochimica Et Biophysica Acta-Biomembranes*, 2006, **1758**, 1292-1302.
19. L. O. Essen, R. Siegert, W. D. Lehmann and D. Oesterhelt, *Proceedings of the National Academy of Sciences of the United States of America*, 1998, **95**, 11673-11678.
20. W. C. Hung, F. Y. Chen, C. C. Lee, Y. Sun, M. T. Lee and H. W. Huang, *Biophysical Journal*, 2008, **94**, 4331-4338.
21. Y. Sun, C. C. Lee, W. C. Hung, F. Y. Chen, M. T. Lee and H. W. Huang, *Biophysical Journal*, 2008, **95**, 2318-2324.
22. E. R. Middleton and E. Rhoades, *Biophysical Journal*, 2010, **99**, 2279-2288.
23. A. J. Trexler and E. Rhoades, *Protein Science*, 2012, **21**, 601-605.
24. B. R. Capraro, Y. Yoon, W. Cho and T. Baumgart, *Journal of the American Chemical Society*, 2010, **132**, 1200-+.
25. A. Tian and T. Baumgart, *Biophysical Journal*, 2009, **96**, 2676-2688.
26. Z. Shi and T. Baumgart, *Advances in Colloid and Interface Science*, 2014.
27. B. R. Capraro, Z. Shi, T. Wu, Z. Chen, J. M. Dunn, E. Rhoades and T. Baumgart, *Journal of Biological Chemistry*, 2013.
28. M. Heinrich, A. Tian, C. Esposito and T. Baumgart, *Proceedings of the National Academy of Sciences of the United States of America*, 2010, **107**, 7208-7213.
29. B. Sorre, A. Callan-Jones, J. Manzi, B. Goud, J. Prost, P. Bassereau and A. Roux, *Proceedings of the National Academy of Sciences of the United States of America*, 2012, **109**, 173-178.
30. T. Wu, Z. Shi and T. Baumgart, *PLoS ONE*, 2014, **9**, e93060.
31. Z. Shi and T. Baumgart, *Nat Commun*, 2015, **6**.
32. T. Baumgart, B. R. Capraro, C. Zhu and S. L. Das, in *Annual Review of Physical Chemistry*, Vol 62, eds. S. R. Leone, P. S. Cremer, J. T. Groves and M. A. Johnson, 2011, vol. 62, pp. 483-506.
33. G. van Meer, D. R. Voelker and G. W. Feigenson, *Nature Reviews Molecular Cell Biology*, 2008, **9**, 112-124.
34. C. G. Sinn, M. Antonietti and R. Dimova, *Colloids and Surfaces A: Physicochemical and Engineering Aspects*, 2006, **282-283**, 410-419.
35. P. Rangamani, K. K. Mandadap and G. Oster, *Biophysical Journal*, 2014, **107**, 751-762.
36. M. Pinot, S. Vanni, S. Pagnotta, S. Lacas-Gervais, L. A. Payet, T. Ferreira, R. Gautier, B. Goud, B. Antony and H. Borelli, *Science*, 2014, **345**, 693-697.
37. R. J. Bruckner, S. S. Mansy, A. Ricardo, L. Mahadevan and J. W. Szostak, *Biophysical Journal*, 2009, **97**, 3113-3122.
38. M. M. Kamal, D. Mills, M. Grzybek and J. Howard, *Proceedings of the National Academy of Sciences of the United States of America*, 2009, **106**, 22245-22250.

-
39. A. R. Braun, M. M. Lacy, V. C. Ducas, E. Rhoades and J. N. Sachs, *Journal of the American Chemical Society*, 2014, **136**, 9962-9972.
40. E. Evans and W. Rawicz, *Physical Review Letters*, 1990, **64**, 2094-2097.
- 5 41. M. Schwarzott, P. Lasch, D. Baurecht, D. Naumann and U. P. Fringeli, *Biophysical Journal*, 2004, **86**, 285-295.
42. I. Szleifer, A. Benshaul and W. M. Gelbart, *Journal of Physical Chemistry*, 1990, **94**, 5081-5089.
- 10 43. S. May, *Soft Matter*, 2009, **5**, 3148-3156.

Figure 1

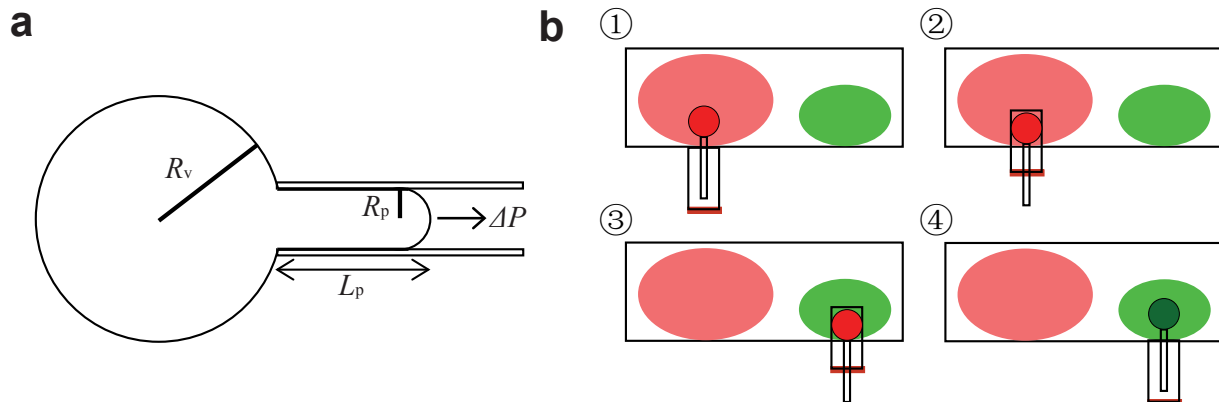


Figure 2

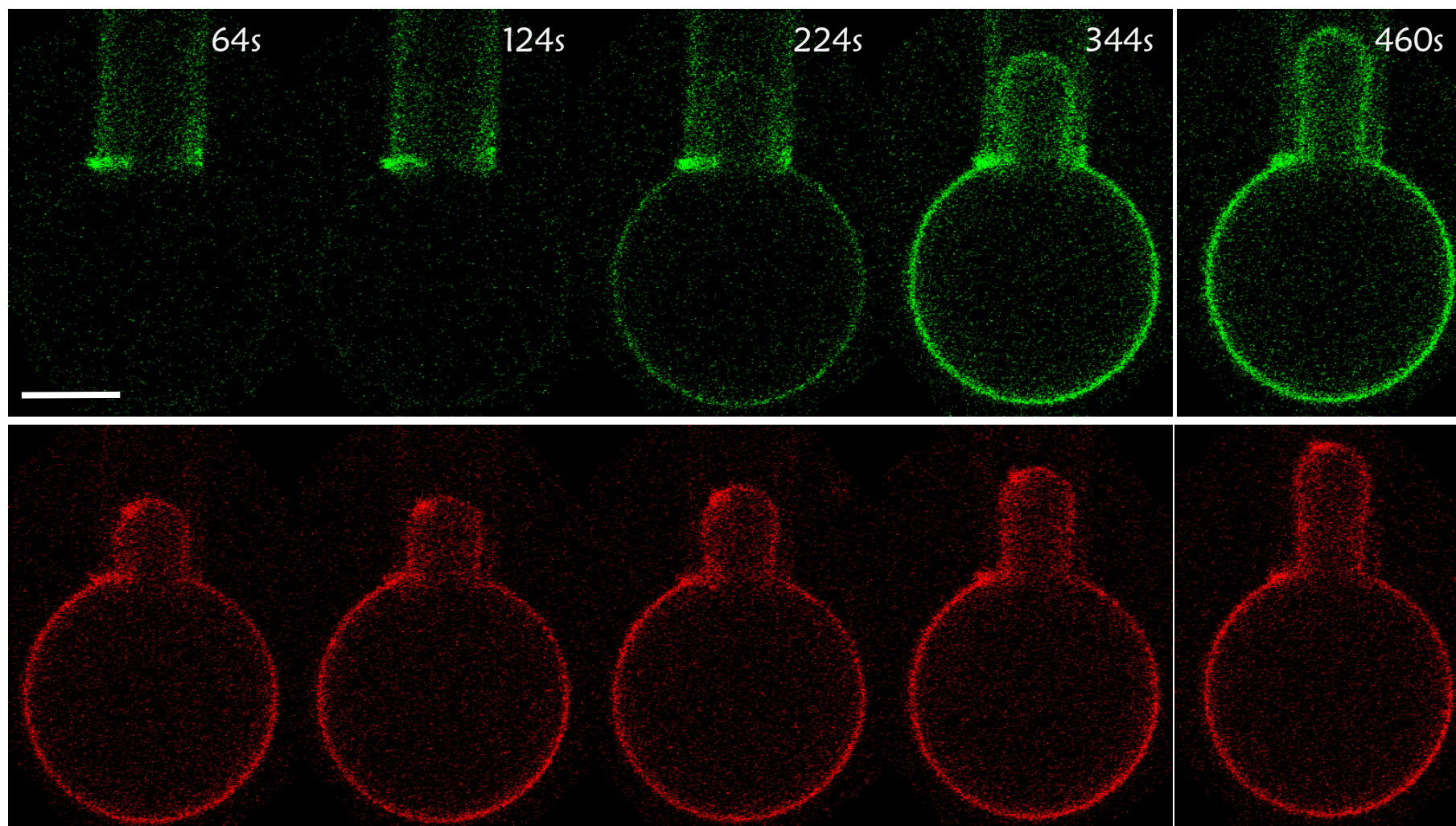
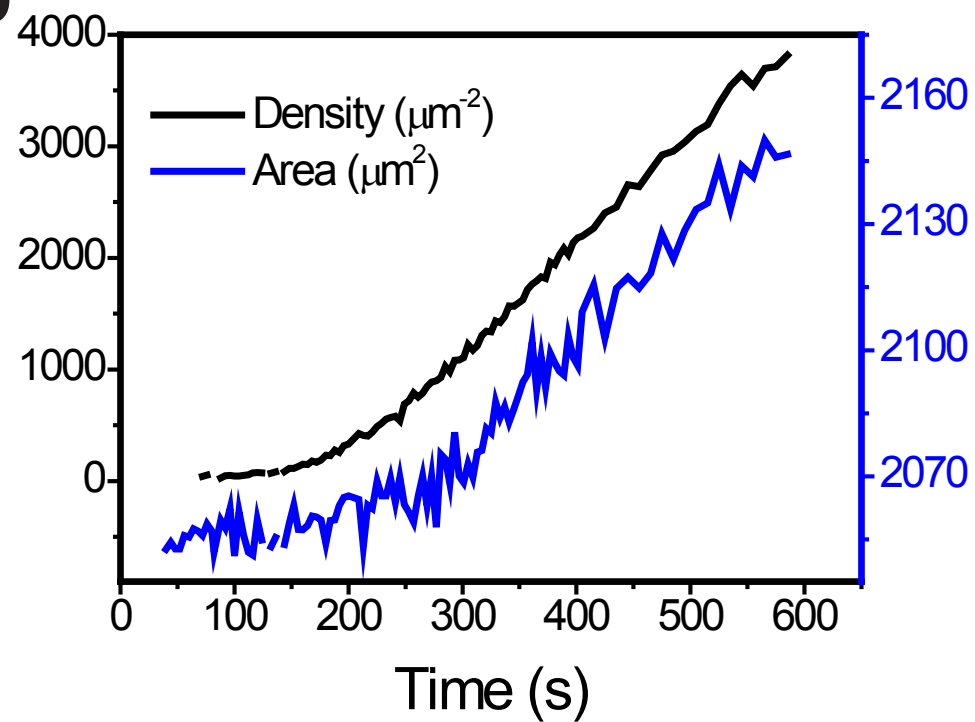
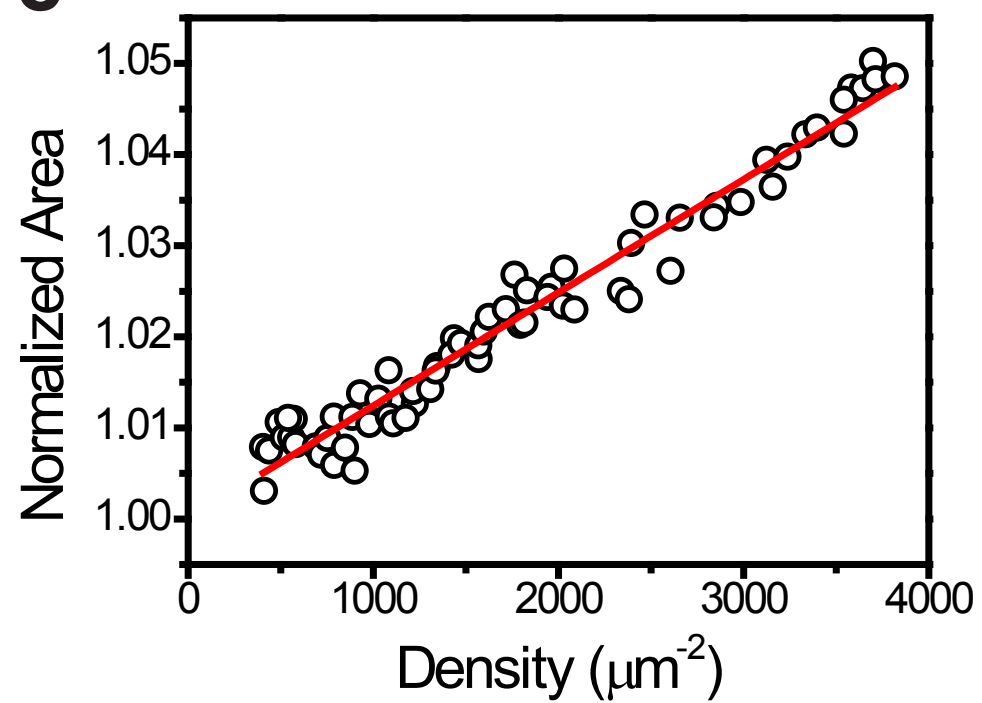
a**b****c**

Figure 3

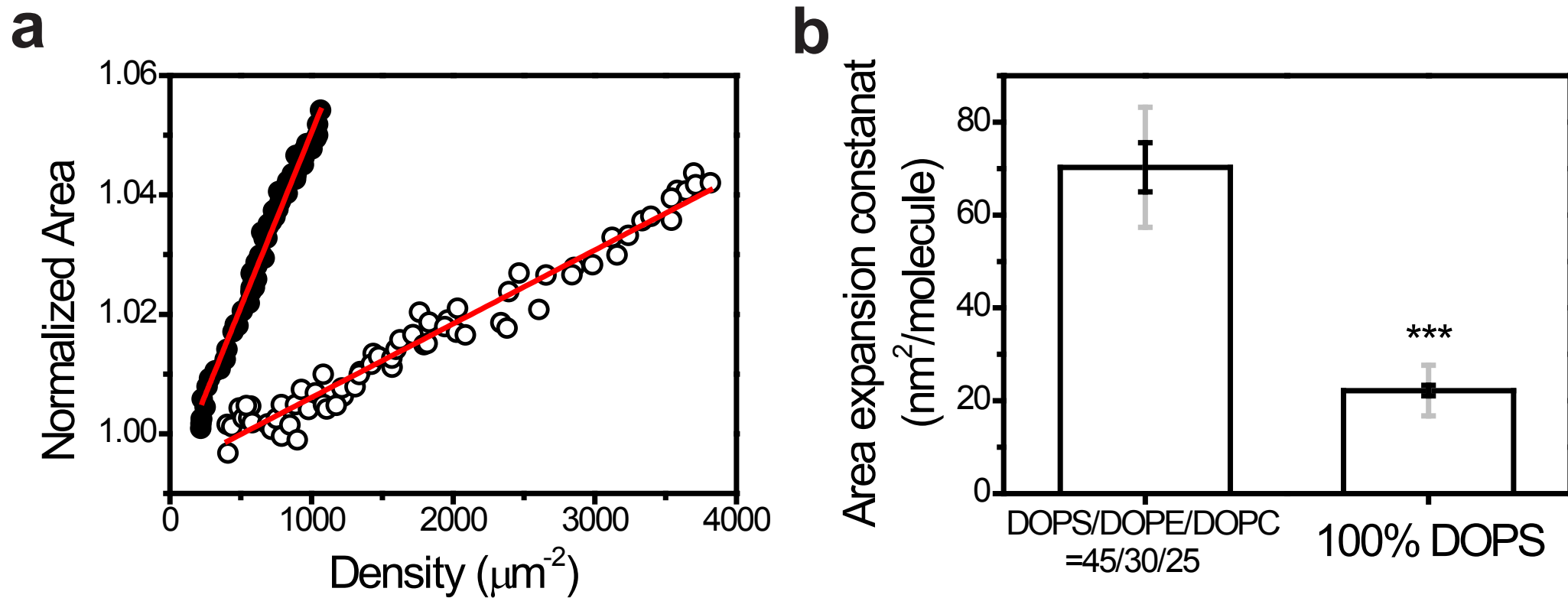


Figure 4

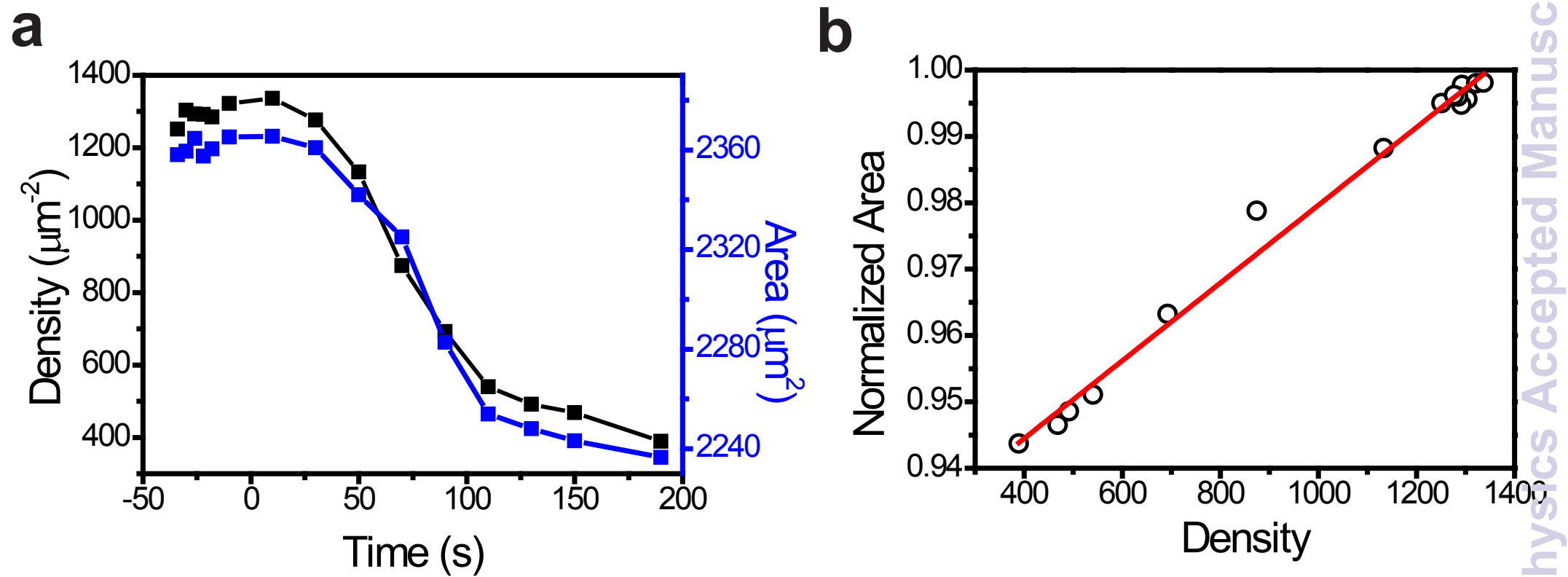


Figure 5

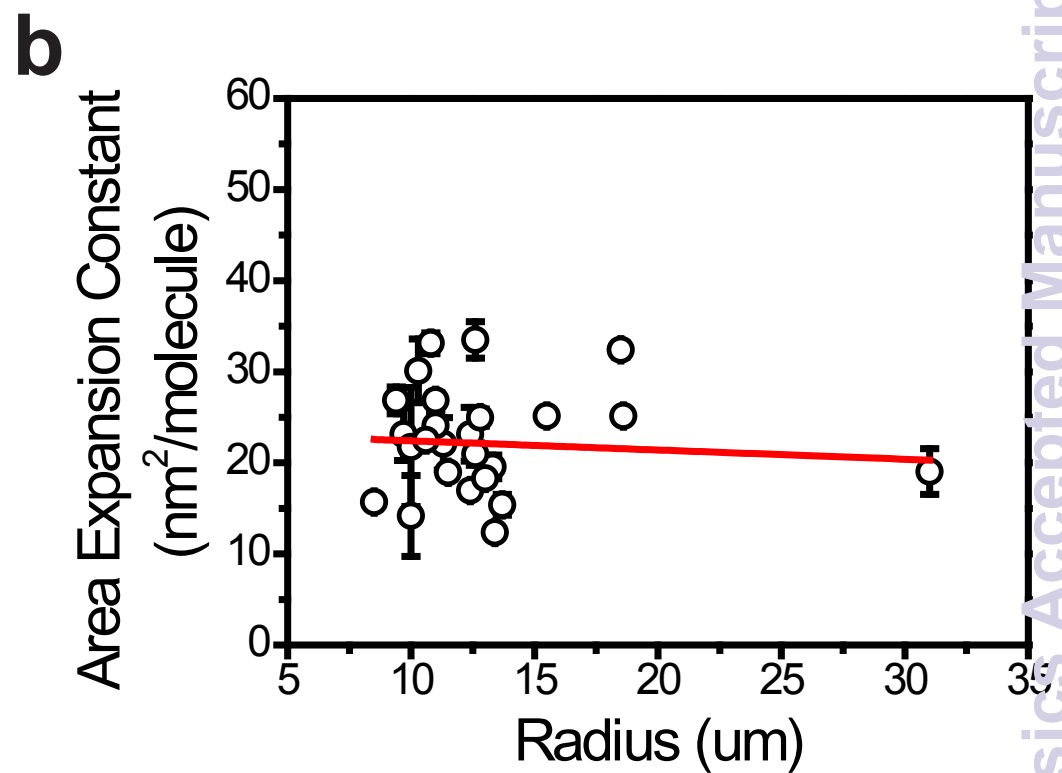
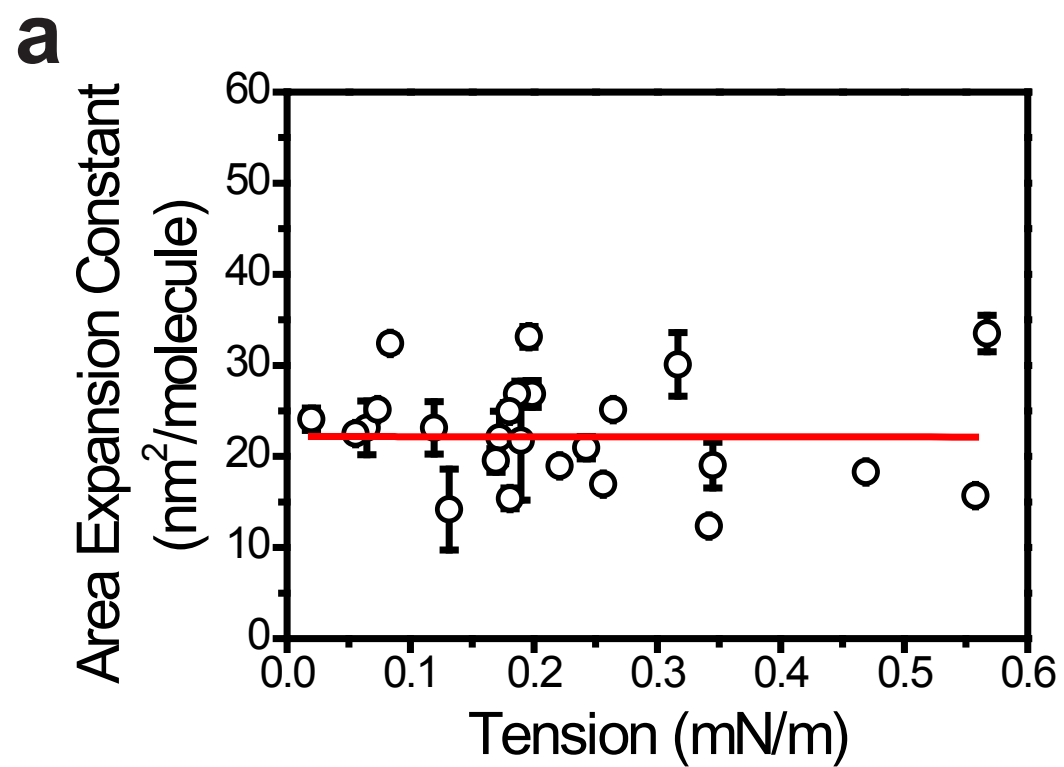


Figure 6

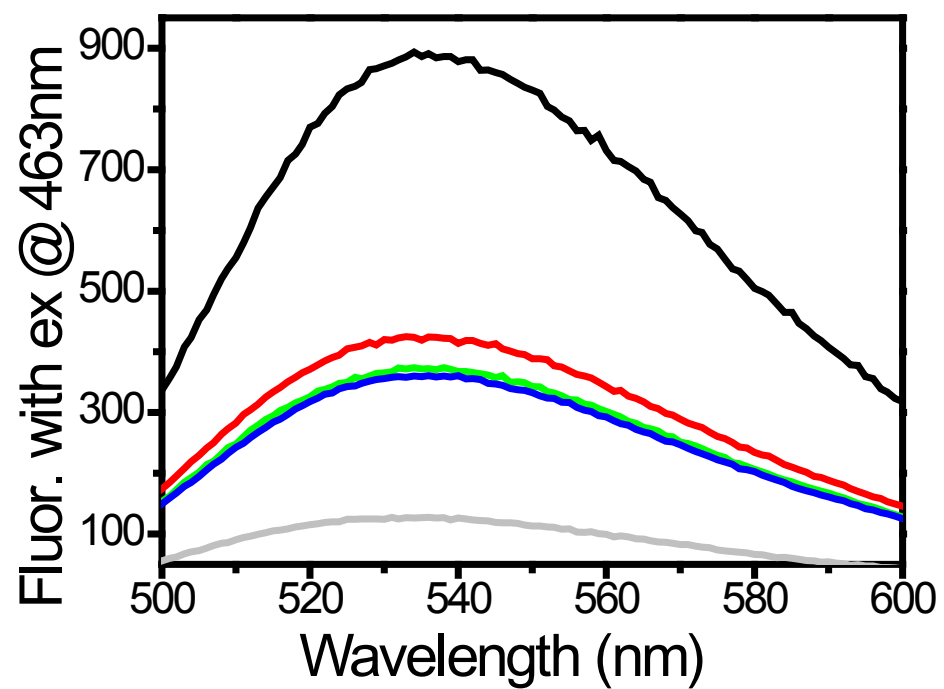
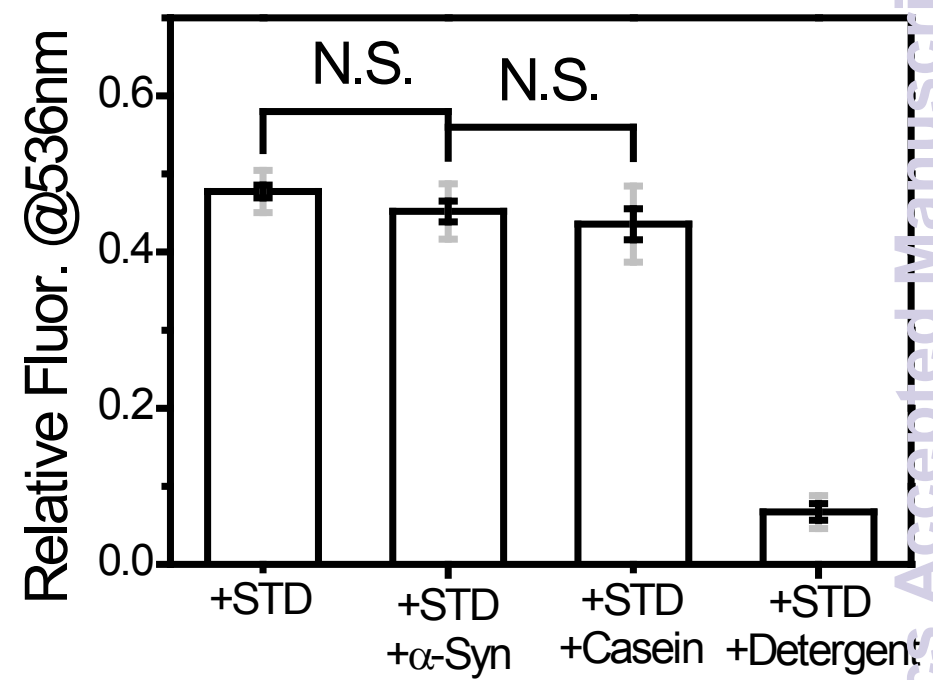
a**b**

Figure 7

